BIOCHEMISTRY
including biophysical chemistry & molecular biology

Article

pubs.acs.org/biochemistry

Activity-Dependent Phosphorylation of Dynamin 1 at Serine 857

Wen Xie,[†,‡,∥] Tatyana Adayev,[‡] Huiyuan Zhu,[‡,⊥] Jerzy Wegiel,[§] Andrzej Wieraszko,[†] and Yu-Wen Hwang*[,‡]

[†]Department of Biology, College of Staten Island, City University of New York, Staten Island, New York 10314, United States
[‡]Department of Molecular Biology and [§]Department of Developmental Neurobiology, New York State Institute for Basic Research in Developmental Disabilities, Staten Island, New York 10314, United States

Supporting Information

ABSTRACT: Dynamin 1 is thought to mediate synaptic transmission through interactions with multiple endocytic accessory proteins in a phosphorylation-dependent manner. Previously, we have shown that DYRK1A, a chromosome 21-encoded kinase implicated in the mental retardation of Down syndrome, phosphorylates primarily serine 857 (S857) in the proline-rich domain, found only in 1xa, one of the alternative C-terminal splicing isoforms of dynamin 1. Dynamin 1xa and 1xb isoforms are able to assemble into heterologous complexes and are coregulated by DYRK1A phosphorylation in binding to amphiphysin in vitro. To help in assessing the physiological significance of S857 phosphorylation, we developed a semiquantitative method for measuring the cellular level of phospho-S857 (pS857). Dynamin 1xa is highly phosphorylated at S857 in resting hippocampal neurons and in a hippocampal cell line, with >60% of all endogenous protein phosphorylated at this residue. In the hippocampus, the level of pS857 is dynamically controlled by synaptic stimulations with the involvement of Ca^{2+}/calcineurin and AMPA/kainate receptors. Immunofluorescence staining shows that pS857 is found in the soma and throughout the entire length of apical dendrites in resting pyramidal neurons. Neuronal stimulation in the Schaffer collateral pathway promotes pS857 dephosphorylation in distal areas of apical dendrites, the region forming synapses with the impinging axons of Schaffer collateral. In summary, our results support the conclusion that S857 phosphorylation is a physiological event and its level is modulated by neuronal activity in nerve terminals.

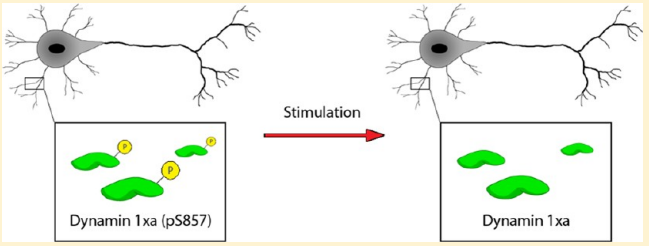

Dynamin 1 is a large (~100 kDa) GTPase[1] that assembles around emerging endocytic vesicles.[2,3] This protein is thought to be directly involved in membrane invagination to form vesicles[4] and in the subsequent severance of the vesicles from the cell membrane.[2,3,5] Dynamin 1 is abundant in the brain[6−8] and is required for mediating both synaptic vesicle recycling and signal transduction from numerous receptors.[1,9]

Dynamin 1 is a phosphoprotein, with the level of phosphorylation tightly regulated by membrane potentials.[10] Phosphodynamin 1, which is maintained at a high level in resting cells, can undergo rapid dephosphorylation upon membrane depolarization, which coincides with the onset of endocytosis. During its functional cycle, dynamin 1 interacts with an array of accessory proteins, such as amphiphysin, endophilin, syndapin, and others to form endocytic complexes, through its C-terminal proline-rich domain (PRD).[11] Dynamin 1 phosphorylation has been shown to regulate these protein−protein interactions.[12−16] Dephosphorylation, which promotes the interactions of dynamin 1 with endocytic accessory proteins, is catalyzed by calcineurin.[10,17] In contrast, multiple kinases, such as cyclin-dependent kinase 5 (Cdk5),[14,18] glycogen synthase kinase 3 (GSK3),[19] and dual-specificity tyrosine phosphorylation-regulated kinase 1A (DYRK1A),[13,15] have been shown to phosphorylate the dynamin 1 PRD.

Cdk5 was shown to phosphorylate the dynamin 1 PRD at S778,[18] which primed a subsequent phosphorylation at S774 by GSK3.[19] Phosphorylation at S774 and S778 affects activity-dependent bulk endocytosis by modulating the interactions of dynamin 1 with syndapin.[16,20] DYRK1A phosphorylates dynamin 1 primarily at S857 in the PRD and regulates the binding of dynamin 1 with several endocytic accessory proteins, including amphiphysin, endophilin, and Grb 2 in vitro.[13,15] The biological consequences of these regulations are still unclear; nevertheless, DYRK1A overexpression has been shown to perturb clathrin-mediated endocytosis by altering the recruitment of endocytic proteins.[21] Dynamin 1 contains three alternative splice sites, one at the middle of the protein (two variants) and the other two at the C-terminus (four variants), which together give rise to eight splicing isoforms, dynamin 1(a,b)(a,b,c,d).[8] The DYRK1A primary phosphorylation site, S857, is found only in the dynamin 1(a,b)(a) (dynamin 1xa) isoforms. Although the level of S857 phosphorylation was shown to be dependent on the membrane potential,[15] the relationship between S857 phosphorylation and physiological activity has not been established. In this study, we show that DYRK1A phosphorylation can modulate the binding of dynamin 1xb, which is lacking S857, to amphiphysin in parallel with dynamin 1xa in vitro. We further

Received: December 2, 2011
Revised: August 1, 2012
Published: August 2, 2012

   dx.doi.org/10.1021/bi2017798 | *Biochemistry* 2012, 51, 6786−6796

demonstrate that S857 of dynamin 1xa is highly phosphorylated in hippocampal neurons and that its level of phosphorylation is controlled by synaptic stimulations.

MATERIALS AND METHODS

Antibodies. Mouse anti-dynamin 1xa phospho-S857 (pS857) antibody 3D3 was described previously.[15] Rabbit anti-dynamin 1 isoform antibodies R24(1xa), R53(1xa), and R56(1xb) were raised against unphosphorylated dynatide 3 (RASPSRPESP-RPPC),[15] a dynamin 1xa-specific peptide (PSRSGQASPSRC), and a dynamin 1xb-specific peptide (GVPRITISDPC), respectively (Figure 1). All rabbit polyclonal antibodies were affinity-purified through the immobilized antigenic peptide before being used. Mouse anti-dynamin antibody Hudy 1 was purchased from Millipore Corp. Alexa Fluor 488-conjugated goat anti-mouse IgG antibody was purchased from Invitrogen (A-11001). Alexa Fluor 568-conjugated antibody 3D3 (3D3-586) was prepared by using the Invitrogen Alexa Fluor 568 Protein Labeling Kit (A-10238), as suggested by the manufacturer. Immunoblotting detection was performed using CDP-Star (New England Biolabs) as previously described.[13] The immobilized antibody was prepared by incubating 50 μL (bed volume) of washed Ultralink protein A/G (Thermo Fisher Scientific) with 10 μg of antibody at 4 °C for 2 h. Coated beads were then blocked with 2% BSA in phosphate-buffered saline with 0.25% Tween 20 (PBST) at 4 °C for 2 h, washed, and stored in 200 μL of PBST with 0.25% sodium azide at 4 °C until use.

Hippocampal Slice Preparation, Stimulation, and Recording. One- to three-month-old CD1 mice were used for the study. Hippocampal slices were prepared, stimulated, and recorded as described previously.[22] Resting slice denoted a slice that was ready for electrophysiological stimulation but had not been exposed to any stimulation. Briefly, stimulation was applied to the CA3 region through a bipolar stimulating electrode, and responses were recorded from the CA1 stratum pyramidale cell layer as population spikes. Three types of stimulation, low-frequency stimulation (LFS), high-frequency stimulation (HFS), and high-frequency plus stimulation (HFS+) (see Figure 4A), were administered. LFS consists of 2 ms stimuli every 30 s for 20 min. HFS consists of three trains of 1 s, 100 Hz stimulation with a 10 s intertrain interval. HFS+ consists of two 10 min LFS flanking an HFS. An elevation of the potential (before and after HFS) by at least 15% for a minimum of 10 min was accepted as long-term potentiation (LTP). Slices to be treated were selected at random from the pool and were incubated in oxygenated Ringer's solution containing the indicated drug at 33 °C for 1 h before the electrophysiological experiments described above were conducted. Drugs were diluted to the working concentration (2 μM cyclosporine, 10 μM BAPTA/AM, 2.5 mM KYA, 50 μM APV, and 50 μM CNQX) and were used immediately. All protocols for animal care and use were approved by the Animal Welfare Committee of the College of Staten Island of the City University of New York.

Extract and Protein Preparation. Acute slice extract was prepared by homogenizing a single hippocampal slice in a disposable micro tissue grinder attached to a motor driver in 50 μL of cold SDS-based lysis buffer [50 mM Tris-HCl (pH 8.0), 20 mM EDTA, 150 mM NaCl, and 0.05% SDS] containing the Complete protease inhibitor cocktail (Roche Diagnostics) and phosphatase inhibitors (0.2 μM okadaic acid, 2 μM cyclosporine A, and 1 mM sodium orthovanadate). After cell debris had been removed by centrifugation (12000*g* for 5 min at 4 °C), the supernatant was saved for subsequent immunological analysis. Synaptosomes were prepared from CD1 mouse hippocampus as described previously.[23] Synaptosomes were then

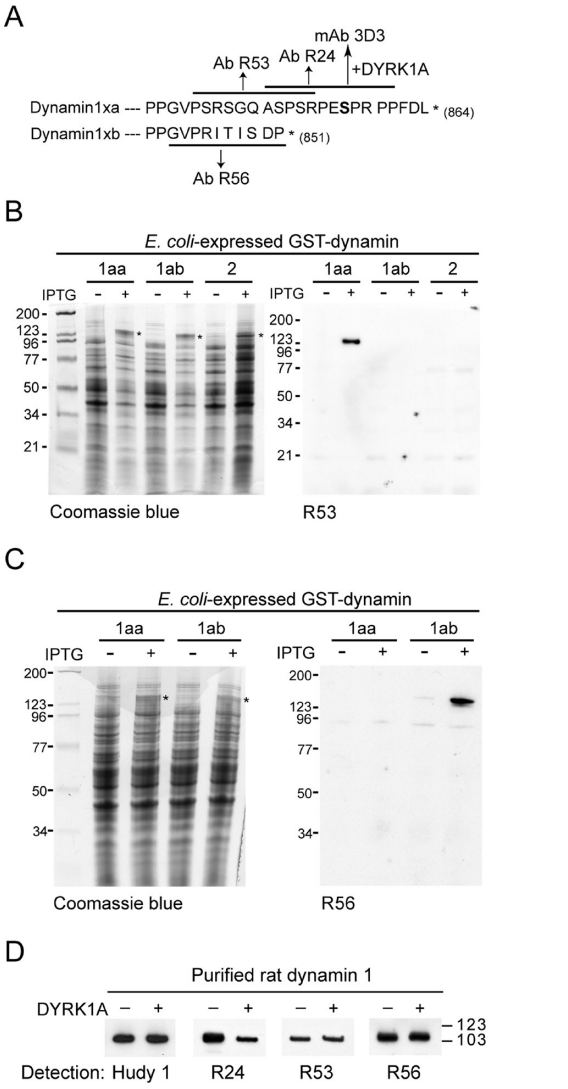

Figure 1. Properties of antibodies R24, R53, and R56. (A) Sequences of antigenic peptides. Peptides (sequence indicated) used for raising antibodies R24, R53, R56, and 3D3 were all derived from the regions near the C-terminal end of dynamin 1xa and 1xb, the region of isoform sequence divergence. Antibodies R24 and 3D3 were raised from the same peptide, dynatide 3,[15] differing in the state of S857 phosphorylation. S857 is shown in bold. (B) Properties of dynamin 1xa-specific antibody R53. Recombinant GST fusion proteins of dynamin 1aa, dynamin 1ab, and dynamin 2 were expressed in *Escherichia coli* (Coomassie blue). The expressed proteins were then subjected to immunoblotting probed with antibody R53. The band corresponding to the full-length GST fusion protein in the Coomassie blue-stained gel is marked with an asterisk. (C) Properties of dynamin 1xb-specific antibody R56. Recombinant GST fusion proteins of dynamin 1aa and 1ab were expressed in *E. coli* (Coomassie blue) probed with antibody R56 exactly as described for panel B. (D) DYRK1A phosphorylation and antibody reactivity. Purified rat brain dynamin 1 was phosphorylated with DYRK1A in vitro and then subjected to immunoblotting with antibodies Hudy 1, R24, R53, and R56 as described in Materials and Methods. The amount of sample used per lane was 50 ng for both unphosphorylated and phosphorylated dynamin 1. −, unphosphorylated dynamin 1; +, DYRK1A-phosphorylated dynamin 1. Antibody Hudy 1 recognizes dynamin 1 in the region around residues 822−838, a region shared by all dynamin 1 isoforms.[26]

dx.doi.org/10.1021/bi2017798 | *Biochemistry* 2012, 51, 6786−6796

incubated in Ringer's solution maintained at 33 °C with oxygenation by constant bubbling of an O_2/CO_2 mixture (95:5) through the solution, to promote dynamin 1 phosphorylation. The synaptosomal samples used for immunoblotting were obtained by boiling synaptosomes in sodium dodecyl sulfate–polyacrylamide gel electrophoresis (SDS–PAGE) loading buffer. HN2-5 lysate was prepared by directly lysing differentiated cells with cold SDS-based lysis buffer supplemented with inhibitors on plate followed by centrifugation (12000*g* for 5 min at 4 °C). Brain Triton extract (BTE) was prepared from adult rat brain without phosphatase inhibitors.[15] Purification of rat brain dynamin 1 was described previously.[13] GST fusion DYRK1A truncated at position 497, as described previously,[24] was used throughout this study.

Phosphorylation, Pull-Down, and Immunological Assays. Purified dynamin 1 was phosphorylated and used for the pull-down assay with the GST fusion amphiphysin 1 SH3 domain as described previously.[13] The molar ratio of DYRK1A to dynamin 1 was adjusted to 1:10 for the phosphorylation reaction (at 30 °C for 30 min) to produce dynamin 1 phosphorylated primarily at S857, as previously described.[15] Dynamin 1 incubated in the absence of DYRK1A was used as the unphosphorylated control. Proteins eluted from the pull-down complexes were then probed with Hudy 1, R53, and R56 by immunoblotting. Immunoprecipitation was conducted by mixing 100 μL (3 mg/mL) of BTE with 10 μL (bed volume, containing 2 μg of antibody) of immobilized antibody at 4 °C overnight. After being washed four times with PBST, precipitated proteins were eluted and probed with an antibody as indicated. For BTE phosphorylation, the extract was incubated with 2 mM ATP and a mixture of phosphatase inhibitors containing 4 μM cyclosporine, 0.2 μM okadaic acid, and 1 mM sodium orthovanadate at 30 °C for 40 min as described previously.[15] Dynatide 3 phosphorylation was performed in a 50 μL reaction mixture containing a kinase buffer [25 mM HEPES (pH 7.5), 100 mM NaCl, and 5 mM $MgCl_2$], 10 μg of dynatide 3, 1 mM ATP, and 1.5 μg of DYRK1A at 30 °C for 60 min. After the first incubation, an additional 1.5 μg of DYRK1A was added to the reaction mixture and incubation was continued at 30 °C for an additional 60 min. Unphosphorylated control dynatide 3 was prepared in parallel but without the addition of DYRK1A. Antibody preabsorption was conducted by incubating 0.5 μg of antibody 3D3-586 with 2 μg of phosphorylated or unphosphorylated dynatide 3 in 20 μL of PBST at room temperature for 2 h. A preabsorption control was similarly prepared by incubating 0.5 μg of antibody with 0.6 μg of DYRK1A.

Determination of the Level of pS857. The level of pS857 was determined as follows. Purified dynamin 1 was phosphorylated with DYRK1A at a molar ratio of 1:4 ([DYRK1A]/[dynamin 1]) for 40 min at 30 °C as described to ensure full phosphorylation at S857.[15] The progress of S857 phosphorylation was monitored at several points by immunoblotting probed with antibody 3D3. The fully phosphorylated dynamin 1 was then mixed with the unphosphorylated material to create a series of pS857 standards with the same dynamin 1 concentration but containing 20, 40, 60, and 80% pS857. Unknown samples to be determined were processed together with all four pS857 standards in the same blot. Tricine/Tris SDS–PAGE with 8% acrylamide (2.6% C) was used for all assays. The amounts of standards (total proteins) to be used were pretested and adjusted to produce an R53 staining intensity comparable to that of the unknown samples. Two identical blots were prepared, one probed with 3D3 and the other with R53. Unphosphorylated dynamin 1 (0%) has consistently not produced a detectable 3D3 signal under our assay conditions. The data for the standards (20–80%) from the 3D3 blot were plotted together with the zero point (0%) and used to fit the sigmoid function $y = a + (b - a)/[1 + (x/c)^d]$ (a, minimum y; b, maximum y; c, x value at midpoint y; d, slope at midpoint y). The apparent pS857 values for the unknown samples were calculated from the curve. The final values were subsequently obtained by correcting the apparent pS857 for the difference in the total amount of dynamin 1xa (from the R53 blot). The relative level of pS857 in stimulated slices (drug-treated or untreated) was determined as follows. An unknown sample was paired with a comparable resting slice and processed together for staining with 3D3 and R53 as described above but without the pS857 standards. The 3D3 ratio for the unknown was first calculated by normalizing the signal of the unknown to that of the resting control (set as 1). The relative level of pS857 was then derived from the 3D3 ratio by correcting it for the difference in the amount of dynamin 1xa (R53 staining). Data are presented as means ± the standard error of the mean, and n represents the number of slices or independent trials analyzed in a given experiment. Statistical evaluations were conducted using one-way ANOVA with Tukey's post hoc analysis. One asterisk and two asterisks denote significant differences at the $p < 0.05$ and $p < 0.01$ levels, respectively.

Immunofluorescence Imaging. Double staining of HN2-5 cells was performed as described below. All procedures were conducted at room temperature unless stated otherwise. Differentiated HN-5 cells were washed once with PBS and fixed with 2% formaldehyde (in PBS) for 20 min followed by incubation in blocking buffer (PBS with 2% BSA, 2% goat serum, and 0.05% saponin) for 1 h. Cells were first incubated with antibody Hudy 1 (2 μg/mL in blocking buffer) for 1 h and then with Alexa Fluor 488-conjugated goat anti-mouse IgG (Invitrogen A-11001, 1:500 dilution) for an additional 1 h to complete the first antibody staining. Afterward, cells were washed three times with PBS (with 0.05% saponin), blocked (1 h), and incubated with antibody 3D3-568 (3 μg/mL in blocking buffer) for 1 h to complete the double staining. Fluorescent images were obtained with a Nikon Eclipse E800 microscope/PCM-2000 confocal system through a Nikon 100×/1.40 Plan Apo objective. For double staining, images for each individual Alexa Fluor dye were captured independently in a single optical section and then merged using Simple PCI software (Nikon). Quantitative colocalization was performed using NIH ImageJ with the JACoP plug-in.[25]

Hippocampal images were stained and captured as follows. Immediately after stimulation, hippocampal slices were fixed in 4% paraformaldehyde at 4 °C for 24 h and then sectioned to 25 μm thicknesses in a cryostat microtome (Vibratome UltraPro 5000) at −20 °C. The sections were blocked in milk buffer (PBS, 2% nonfat dry milk, 0.2% Triton X-100, and 10% goat serum) for 1 h before being incubated with the primary antibody (3D3 at 2.5 μg/mL or Hudy 1 at 2 μg/mL, diluted in milk buffer) at 4 °C overnight. The next day, the sections were rinsed three times with PBS, blocked with milk buffer for 1 h, and then incubated with Alexa Fluor 488-conjugated goat anti-mouse IgG antibody (1:500 dilution in milk buffer) for an additional 1 h. After being extensively washed with PBS, the sections were mounted on gelatin-coated slides with an antifade

reagent for confocal microscopy examination. Fluorescence images were acquired with a Nikon Eclipse 90i microscope-equipped D-Eclipse C1 confocal system. The objective used was either a Nikon Plan Apo 40×/1.0 (for 3D3 staining) or 20×/0.75 lens (for Hudy 1 staining). A sequence of 30−40 sections in a 0.6 μm step was obtained using successive z-scans, which were subsequently combined to produce z-stack projections using AutoDeblur and AutoVisualize.

RESULTS

Measuring the Level of Dynamin 1xa S857 Phosphorylation in Vivo. To assess whether dynamin 1xa S857 phosphorylation is physiologically significant, we developed a semiquantitative immunoblotting-based method to measure the level of dynamin 1xa S857 phosphorylation in vivo. The assay requires two specific antibodies, one for quantifying phospho-S857 (pS857) and one for total dynamin 1xa protein. The specific pS857 antibody, 3D3, has been described previously.[15] Antibodies for quantifying dynamin 1xa were prepared and characterized in this study (Figure 1A). Dynamin 1 contains multiple isoforms,[8] and samples from different sources were to be analyzed. Therefore, the quantifying antibody must demonstrate both of the following criteria: (1) specificity toward the dynamin 1xa isoform and (2) S857 phosphorylation-independent immunoreactivity. Our results show that although both antibodies R53 (Figure 1B) and R24 (data not shown) were specific for detecting the dynamin 1xa isoform, only R53 was suitable for the assay because its immunoreactivity was independent of S857 phosphorylation (Figure 1D). The well-characterized dynamin 1 antibody Hudy 1[26] reacted with multiple dynamin 1 isoforms (data not shown); therefore, it was also not usable for the assay. An antibody specific for dynamin 1xb, R56, was similarly prepared and characterized (Figure 1A,C). Like all other antibodies depicted in Figure 1A, R56 also reacted with purified rat brain dynamin 1, and the immunoreactivity of R56 was unaffected by S857 phosphorylation (Figure 1D). R56 has a specificity profile identical to that of the anti-dynamin 1(xb) antibody published previously by others.[7]

Briefly, the level of pS857 was measured as follows. Purified native rat brain dynamin 1 (containing at least the dynamin 1xa and 1xb isoforms) was phosphorylated extensively with DYRK1A until the level of pS857 had plateaued (Figure 1A). S857 phosphorylation at this stage is essentially stoichiometric if the reaction is performed with sufficient kinase ([DYRK1A]/[dynamin 1] ≥ 1/10).[13,15] The fully phosphorylated dynamin 1 (100%) was mixed with the unphosphorylated protein (0%) to create a series of pS857 standards (0−100%). 3D3 immunoreactivity increased in a pS857 level-dependent manner, and the response throughout the entire range of pS857 (Figure 2B) was fit to the sigmoid function described in Materials and Methods. For determining the unknowns, samples to be analyzed were processed together with a set of standards containing 20−80% pS857 in two separate immunoblots: one probed with pS857-specific antibody 3D3 (Figure 2C,D) and the other with dynamin 1xa-specific antibody R53 (Figure 1). The apparent level of pS857 was calculated from the pS857 standard curve from the 3D3 blot and then corrected for the total amount of dynamin 1xa used in the assay to derive the final level.

We measured the level of pS857 in hippocampal cell line HN2-5,[27] acute hippocampal slices, rat brain Triton extract (BTE), and synaptosomes. HN2-5 cells express sufficient dynamin 1xa for detection, and its level can be further increased upon terminal neuronal differentiation induced by retinoic acid.

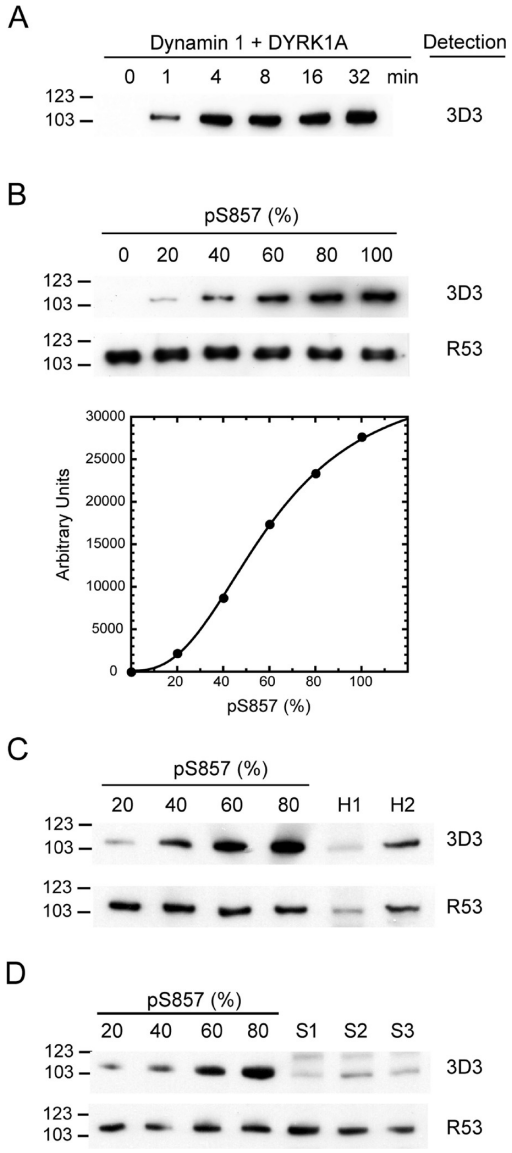

Figure 2. Determination of the level of pS857. (A) Time course phosphorylation of purified dynamin 1 at S857 by DYRK1A. Dynamin 1 was phosphorylated with DYRK1A with a molar ratio of 4:1 as described in Materials and Methods. Phosphorylated dynamin 1 was withdrawn at the indicated time points and analyzed for pS857 by immunoblotting with antibody 3D3. (B) pS857 levels and 3D3 immunoreactivity. A set of six standards containing 0, 20, 40, 60, 80, or 100% pS857 were prepared and probed with antibodies 3D3 and R53. The immunoreactivity of each standard was quantified and plotted vs the level of pS857. The data were fit with the sigmoid function described in Materials and Methods. (C) Determination of the level of pS857 in acute slice. The extract (acute slice) to be analyzed was prepared from a single resting hippocampal slice in the presence of phosphatase inhibitors. The resulting extract was then processed together with four standards with known pS857 levels (from 20 to 80%) for immunoblotting with antibodies 3D3 and R53 to determine the level of pS857 as described in Materials and Methods. H1 and H2 were two different acute slice samples. (D) Determination of the level of pS857 in synaptosomes. The level of pS857 in the synaptosomal extract was determined exactly as described above. S1, S2, and S3 were synaptosomes that had been incubated in oxygenated Ringer's solution for 0, 15, and 60 min, respectively, before lysis.

dx.doi.org/10.1021/bi2017798 | *Biochemistry* 2012, 51, 6786−6796

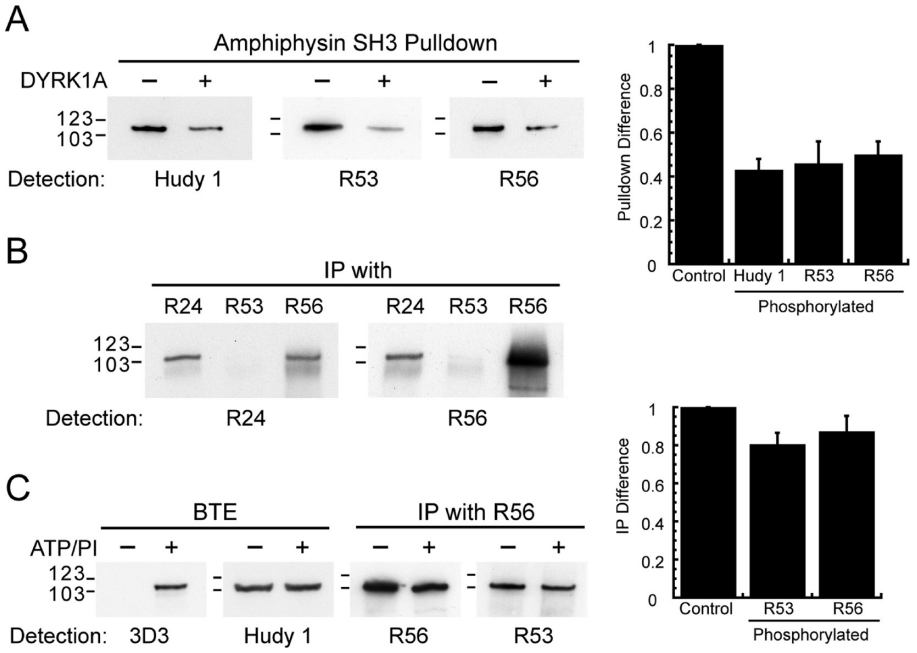

Figure 3. Coregulation of dynamin 1 isoforms by S857 phosphorylation. (A) Effect of DYRK1A phosphorylation on binding of dynamin 1 isoforms to the amphiphysin 1 SH3 domain. Dynamin and amphiphysin binding was measured by the pull-down assay described in Materials and Methods. The level of total dynamin 1, 1xa, and 1xb (R56) isoforms in the pull-down complexes was analyzed using antibody Hudy 1, R53, and R56, respectively. −, control unphosphorylated dynamin 1; +, dynamin 1 phosphorylated with DYRK1A. A set of representative blots is shown. The ratio of pull-down difference between phosphorylated and unphosphorylated control (set as 1) dynamin 1 was calculated for each antibody, and data from three trials were plotted. The ratios of pull-down difference for total dynamin (Hudy 1; $n = 3$), dynamin 1xa (R53; $n = 3$), and dynamin 1xb (R56; $n = 3$) were statistically evaluated [$F(2,6) = 0.27$; $p = 0.77$]. (B) Co-immunoprecipitation of dynamin 1 isoforms from BTE. Immunoprecipitation was first conducted with the antibody indicated on the top of the blot (R24, R53, and R56) from untreated BTE as described in Materials and Methods. Proteins eluted from the immunoprecipitation complexes were then probed for dynamin 1xa (R24) and dynamin 1xb (R56). A set of representative blots from multiple trials is shown. (C) Effects of S857 phosphorylation on dynamin 1 isoform co-immunoprecipitation. BTE was prepared and treated with ATP and phosphatase inhibitors (ATP/PI "+") as described. Untreated control (ATP/PI "−") was similarly prepared but without the addition of ATP and phosphatase inhibitors. The resulting extracts and were either probed with antibody 3D3 or Hudy 1 or used for immunoprecipitation using antibody R56 as described above. Proteins eluted from the immunoprecipitation complexes were then analyzed for dynamin 1xb (R56) and dynamin 1xa (R53). A set of representative blots is shown. The ratio of immunoprecipitation difference before and after phosphorylation was calculated for each dynamin isoform by dividing the level of immunoprecipitation from treated BTE (phosphorylated) by that from the untreated BTE (control, set as 1) performed in parallel. The plot represents the data from three trials. The ratios of immunoprecipitation difference for dynamin 1xa (R53; $n = 3$) and dynamin 1xb (R56; $n = 3$) were statistically evaluated [$F(1,5) = 0.28$; $p = 0.62$].

HN2-5 extract was obtained by directly lysing differentiated cells on plates. The acute slice extract was prepared from a single resting slice, and the material was equivalent to that of resting samples shown in Figures 4 and 5. The synaptosomal extract was prepared from mouse hippocampal synaptosomes, which were preincubated in oxygenated Ringer's solution for 15 and 60 min after synaptosome preparation. Dynamin 1xa was highly phosphorylated at S857 in the resting acute slice, reaching a level of >60% (65.9 ± 5.8%; $n = 5$). S857 was also highly phosphorylated in HN2-5 cells (67.0 ± 6.5%; $n = 3$). In contrast, little pS857 was found in fresh synaptosomal dynamin 1xa (7.3 ± 1.6%; $n = 3$), and the level was not substantially elevated even with prolonged incubation of synaptosomes in Ringer's solution (9.5 ± 1.3 and 12.6 ± 3.0% with incubation for 15 and 60 min, respectively; $n = 3$). The inability to support a substantial level of dynamin 1xa S857 phosphorylation in synaptosomes is consistent with the finding that pS857 is a minor component of the total dynamin 1 phosphorylation in synaptosomes.[28,29] Addition of phosphatase inhibitors during lysate extraction is required for the preservation of pS857. Without inhibitors, extracts contain no detectable pS857. We have previously found that pS857-depleted BTE can regain pS857 levels upon incubation with ATP and phosphatase inhibitors in vitro[15] (see also Figure 3C). Here, we show that the level of S857 phosphorylation can reach ∼40% (40.6 ± 4.1%; $n = 3$) after incubation for 40 min, as measured by the method described above.

DYRK1A Phosphorylation Coregulates the Interactions of Dynamin 1 Isoforms with the Amphiphysin SH3 Domain. DYRK1A phosphorylation was shown to alter the interactions of dynamin 1 with various SH3 domain-containing endocytic proteins in vitro.[13,15] Because the primary phosphorylation site of DYRK1A is unique to the 1xa isoform[8] and we have previously used antibody Hudy 1 for detection,[13,15] it has been assumed that the consequences of DYRK1A phosphorylation are solely associated with the 1xa isoform.[15] Additional antibodies offer an opportunity to reexamine the effects of DYRK1A phosphorylation in an isoform-specific manner. Purified native rat brain dynamin 1 was phosphorylated by DYRK1A, and each isoform was analyzed for changes in the pull down with amphiphysin SH3 domain protein (Figure 3A). Here, we confirm that the level of binding of dynamin 1xa to amphiphysin is reduced by DYRK1A phosphorylation in vitro (Figure 3A, R53). Our result further shows that the level of binding of dynamin 1xb to amphiphysin is also similarly reduced by DYRK1A phosphorylation (Figure 3A, R56), although the

dx.doi.org/10.1021/bi2017798 | Biochemistry 2012, 51, 6786−6796

isoforms do not contain the major DYRK1A phosphorylation site.

Dynamin is known to self-assemble,[2,30] and distinct isoforms may be incorporated into the same protein complex.[31] One possible explanation for this observation is that dynamin 1xa and 1xb form heterologous complexes and are coprecipitated by immobilized amphiphysin. We subsequently examined heterologous complex formation in vitro by co-immunoprecipitation (co-IP). A dynamin 1 isoform was first precipitated from rat BTE (prepared without phosphatase inhibitors) with an isoform-specific antibody, and the precipitated complexes were then probed for the other isoform by immunoblotting. The results in Figure 3B confirm co-IP of dynamin 1xa and 1xb in a reciprocal fashion regardless of which isoform precipitated first (Figure 3B, R24 and R56). On the other hand, antibody R53, which is unable to precipitate dynamin 1xa and therefore is useful as a negative control, was unable to precipitate dynamin 1xb (Figure 3B). We further analyzed whether S857 phosphorylation altered heterologous dynamin 1 complex formation by comparing the level of isoform co-IP between the control extract (pS857-depleted) and the extract incubated with ATP and phosphatase inhibitors (ATP/PI). The ATP/PI treatment significantly elevated the level of pS857 (Figure 3C, 3D3) but had little effect on dynamin 1xb IP (Figure 3C, R56) or dynamin 1xa co-IP with dynamin 1xb (Figure 3C, R53). This result suggests that dynamin 1 heterologous complex formation is independent of S857 phosphorylation. The reciprocal IP was not performed because antibody R24 proved to be sensitive to S857 phosphorylation (Figure 1D). The formation of heterologous complexes also explains the constant detection of both dynamin 1xa and 1xb in purified rat brain dynamin 1 (Figure 1D).

Regulation of Dynamin 1xa S857 Phosphorylation by Hippocampal Activity. The state of S857 phosphorylation is linked to membrane potential in cultured cells; membrane depolarization promotes the reduction of pS857.[15] Thus, we investigated whether the level of pS857 in hippocampus was subject to regulation by hippocampal synaptic activity. We employed the standard acute hippocampal slice stimulation paradigm for inducing synaptic transmission in the Schaffer collaterals by administering one of the following stimulation protocols, low-frequency stimulation (LFS), high-frequency stimulation (HFS), and high-frequency plus stimulation (HFS+) (Figure 4A), at the CA3 region of the hippocampus. Stimulated slices were frozen immediately in a dry ice/ethanol bath and then processed to determine the level of pS857 relative to those of the resting (unstimulated) slices (Figures 4 and 5, Resting).

LFS did not produce a significant change in the steady-state level of pS857 (0.96 ± 0.13, $n = 6$, $p = 0.99$ vs the resting slices) (Figure 4B). In contrast, the level of pS857 was drastically reduced (0.29 ± 0.05, $n = 6$, $p < 0.01$ vs the resting slices) upon HFS. HFS+, which includes LFS following HFS, was also found to reduce pS857 (0.69 ± 0.05, $n = 17$, $p = 0.02$ vs the resting slices); however, the resulting level was significantly higher than that of the HFS-stimulated slices ($p < 0.01$) (Figure 4B). It is possible to observe the induction of long-term potentiation (LTP)[32] in the second LFS phase of HFS+; therefore, HFS+-stimulated slices were further divided into two subgroups on the basis of actual LTP expression. The level of dynamin 1xa pS857 in the LTP group was higher than that in the non-LTP group (0.77 ± 0.06, $n = 10$, vs 0.58 ± 0.06, $n = 7$, $p < 0.05$) (Figure 4B). Together, the results demonstrate that the level of pS857 in hippocampus is dynamically regulated by neuronal activity. HFS readily promotes pS857 dephosphorylation, and a period of LFS allows substantial rephosphorylation of S857, especially when LTP is established.

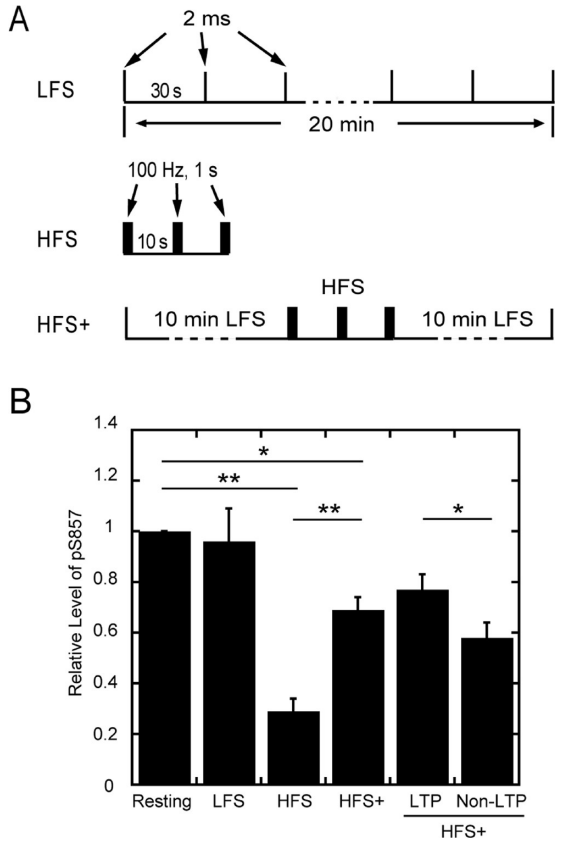

Figure 4. Stimulation of dynamin 1xa pS857 dephosphorylation in hippocampal slices. (A) Diagrams of three types of stimulation used in the study. The drawings (not to scale) depict the frequency and duration for each stimulation: LFS, 2 ms (ms) stimuli every 30 s (s) for 20 min; HFS, three trains of 1 s, 100 Hz stimulation with a 10 s interval; HFS+, LFS for 10 min, HFS, and LFS for 10 min. (B) Relative level of dynamin 1xa pS857 in stimulated hippocampal slices. Slices were stimulated as indicated. The level of phosphorylation of S857 in each stimulated slice was then determined in parallel with a resting slice (set as 1) to deduce the relative pS857 level as described in Materials and Methods. Resting, LFS, HFS, and HFS+ were statistically evaluated [$F(3,31) = 15.89$; $p < 0.01$]. LTP and Non-LTP slices in the HFS+ group were further compared [$F(1,15) = 4.61$; $p < 0.05$]. One asterisk and two asterisks indicate the significant differences in pairwise comparisons at the $p < 0.05$ and $p < 0.01$ levels, respectively.

Role of Ca^{2+}/Calcineurin and Ionotropic Glutamate Receptors in Dynamin 1xa pS857 Dephosphorylation. We investigated whether Ca^{2+}/calcineurin was involved in pS857 dephosphorylation in hippocampus. Hippocampal slices were preincubated with either calcineurin inhibitor cyclosporine (CS) or calcium chelator BAPTA/AM, exposed to HFS, and then analyzed for their level of pS857. Neither CS nor BAPTA/AM significantly altered the pS857 level in resting slices, but HFS-stimulated pS857 dephosphorylation was eliminated by either CS (0.90 ± 0.10, $n = 7$, $p = 0.02$ vs HFS) or BAPTA/AM (1.07 ± 0.21, $n = 7$, $p < 0.01$ vs HFS) (Figure 5A). These results indicate that pS857 dephosphorylation in hippocampus requires Ca^{2+}/calcineurin.

dx.doi.org/10.1021/bi2017798 | *Biochemistry* 2012, 51, 6786–6796

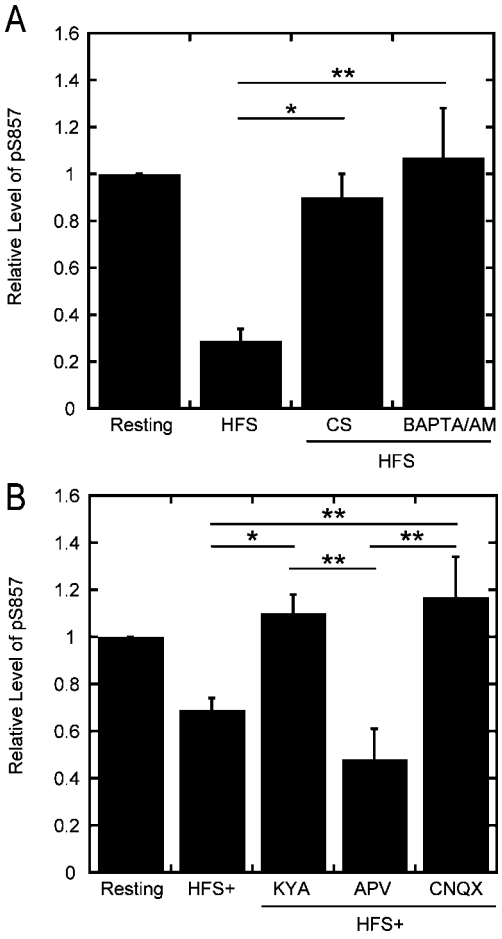

Figure 5. Involvement of Ca^{2+}/calcineurin and ionotropic glutamate receptors in stimulated pS857 dephosphorylation. (A) Ca^{2+}/calcineurin. Slices were preincubated with the indicated 2 μM cyclosporine (CS) or 10 μM BAPTA/AM in oxygenated Ringer's solution at 33 °C for 60 min and then subjected to HFS. The relative pS857 level of each slice (normalized to that of a drug-treated resting slice) was determined as described in Materials and Methods. HFS data were the same data as in Figure 4B. HFS, CS, and BAPTA/AM were statistically evaluated [$F(2,17) = 7.96$; $p < 0.01$]. (B) Ionotropic glutamate receptors. Slices were preincubated with the indicated compound (2.5 mM for KYA, 50 μM for APV, or 50 μM for CNQX) in oxygenated Ringer's solution at 33 °C for 60 min, stimulated with HFS+, and then processed to determine the relative pS857 level (normalized to that of a drug-treated resting slice) as described in Materials and Methods. HFS+ data were the same data as in Figure 4B. HFS+, KYA, APV, and CNQX were statistically evaluated [$F(3,30) = 9.99$; $p < 0.01$].

As the neuronal activity in the Schaffer collateral−CA1 pathway is mediated primarily by the activation of ionotropic glutamate receptors,[33] we further examined the role of these receptors in pS857 dephosphorylation. Slices were pretreated with kynurenic acid (KYA), a general ionotropic glutamate receptor antagonist, and analyzed as described. KYA-treated slices did not display population spikes. The drug eliminated HFS+-promoted pS857 dephosphorylation (1.10 ± 0.08, $n = 6$, $p = 0.01$ vs HFS+) (Figure 5B) without affecting resting levels of pS857. Two selective antagonists, 6-cyano-7-nitroquinoxaline-2,3-dione (CNQX), an AMPA/kainate receptor antagonist, and D-2-amino-5-phosphonopentanoic acid (APV), a NMDA receptor antagonist, were subsequently employed to distinguish the subtypes of ionotropic glutamate receptors involved in pS857 dephosphorylation. Slices treated with CNQX did not exhibit detectable population spikes, while slices treated with APV displayed population spikes but failed to express LTP. Neither drug altered the basal pS857 level. Nevertheless, pS857 dephosphorylation promoted by HFS+ was blocked by CNQX (1.17 ± 0.17, $n = 6$, $p < 0.01$ vs HFS+) but not by APV (0.48 ± 0.13, $n = 5$, $p = 0.39$ vs HFS+) (Figure 5B). These results suggest that dephosphorylation of pS857 is primarily mediated by the AMPA/kainate receptors.

Regulation of the Distribution of pS857 in Hippocampus. The cellular distribution of pS857 dynamin 1xa was subsequently examined by immunofluorescence staining with antibody 3D3. We first compared antibodies 3D3 and Hudy 1 in staining of differentiated HN2-5 cells. Hudy 1 stained punctate vesicle-like structures, which were concentrated in the cell periphery and neurite extensions (Figure 6A and Figure S1 of the Supporting Information). This pattern of Hudy 1

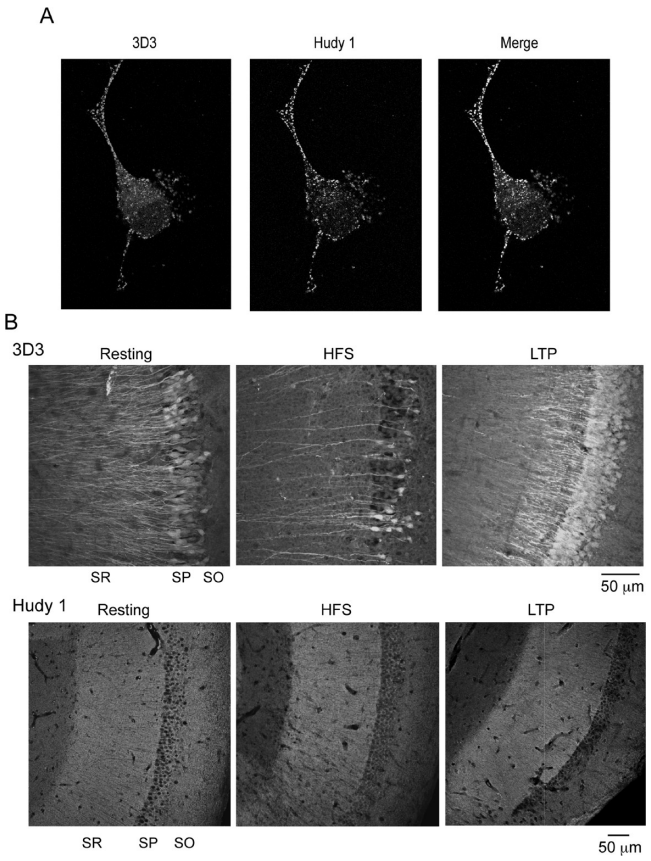

Figure 6. Subcellular distributions of pS857 dynamin 1xa and dynamin 1. (A) Distributions of pS857 dynamin 1xa (3D3) and dynamin 1 (Hudy 1) in differentiated HN2-5 cells. Cells were cultured, differentiated, doubly stained with 3D3-568) and Hudy 1 (Alexa Fluor 488), visualized, and quantified as described in Materials and Methods. Color versions of these three panels appear in the Supporting Information (Figure S1). The images produced a Pearson's coefficient of 0.744 and an intensity correlation quotient of 0.412. (B) Distributions of pS857 dynamin 1xa in the CA1 region of stimulated hippocampus. Slices were stimulated as indicated and then probed with antibody 3D3 (top) or Hudy 1 (bottom) as described in Materials and Methods. The CA1 region of the hippocampus is shown. Abbreviations: Resting, control slice; HFS, slice stimulated with HFS; LTP, LTP-expressing slice; SR, stratum radiatum; SP, stratum pyramidale; SO, stratum oriens. Color versions of these six panels appear in the Supporting Information (Figure S3).

dx.doi.org/10.1021/bi2017798 | *Biochemistry* 2012, 51, 6786−6796

staining is consistent with numerous published observations.[34,35] The localizations of pS857 dynamin 1xa were found to overlap largely with that of dynamin 1 detected by antibody Hudy 1 (Figure 6A and Figure S1 of the Supporting Information). The conclusion is supported by quantitative analysis of colocalization (see the legend of Figure 6A). Further analysis using antibody 3D3 preabsorbed with DYRK1A-phosphorylated dynatide 3[15] suggests that the structures stained by antibody 3D3 indeed contain the epitope corresponding to the portion of the C-terminus of dynamin 1xa containing pS857 (Figure S2 of the Supporting Information). The costaining reflects the finding that different dynamin 1 isoforms form heterologous complexes as suggested by co-IP (Figure 3B). It also indicates that Hudy 1 staining can be used for visualizing dynamin 1xa on the cellular level. Antibody R53 was unable to produce satisfactory immunofluorescence staining of cells and hippocampal sections and thus was not used in this study.

3D3 appeared to stain most pyramidal neurons, especially in the CA1 regions. The cellular distribution of pS857 dynamin 1xa was polarized in pyramidal neurons in the resting hippocampus. Dynamin 1xa pS857 was abundant in soma and in the entire length of apical dendrites in the region of stratum radiatum (Figure 6B and Figure S3 of the Supporting Information). On the other hand, little pS857 was found in basal dendrites (Figure 6B). The distribution of pS857 in apical dendrites was similar to that of dendritic marker MAP2.[36] Upon HFS, the number of pS857 positive neurons was drastically reduced compared to the number of unstimulated resting slices. Antibody 3D3 staining was completely eliminated from the affected neurons (Figure 6B). However, the staining patterns were essentially unchanged for a few unaffected neurons. This result suggests that HFS reduced the pS857 level (Figure 4B) in stimulated slices in a global all-or-nothing fashion. In contrast, LTP produced an apparent redistribution of pS857 dynamin 1xa without affecting the total number of 3D3-stained neurons. Specifically, 3D3 staining in distal apical dendrites was largely eliminated during LTP (Figure 6B). As a consequence, pS857 was now restricted to soma and to proximal areas of apical dendrites. Even with the apparent redistribution, 3D3 staining was still weak in basal dendrites. The change in 3D3 staining patterns could be attributed to the regional dephosphorylation of pS857 in distal apical dendrites or to the actual relocation of dynamin 1xa. To distinguish these two possibilities, we probed stimulated slices with antibody Hudy 1. No apparent changes, particularly for stratum radiatum, in Hudy 1 staining patterns were observed among the resting, HFS-stimulated, and LTP slices (Figure 6B). These results suggest that the apparent pS857 redistribution is caused by regional dephosphorylation of pS857 in distal apical dendrites during LTP, rather than by dynamin 1xa relocation.

DISCUSSION

A semiquantitative method for measuring the level of pS857 dynamin 1xa in vivo is described. The method allows us to determine pS857 levels in hippocampal cells, synaptosomes, and the procedure can be easily applied under a variety of conditions. Dynamin 1xa, in the resting hippocampus and neuronal cell lines, is highly phosphorylated at S857, with >60% of the total cellular protein being phosphorylated at this residue (Figure 2). Our conclusion that S857 is a major in vivo phosphorylation site is in agreement with results from proteomic analysis of brain dynamins.[29] The involvement of such a large proportion of total dynamin 1xa suggests that S857 phosphorylation is likely a physiological event. The physiological significance of S857 phosphorylation is further strengthened by the finding that pS857 is dynamically regulated by hippocampal synaptic activity (Figure 4B) with the participation of Ca^{2+}/calcineurin and AMPA/kainate receptors (Figure 5). HFS, which is routinely used to promote LTP,[32] caused an acute pS857 reduction of ~70% from that of resting slices (Figure 4B). In contrast, slices stimulated with HFS+, a stimulation consisting of LFS, HFS, and LFS, possessed a surprisingly high steady-state level of pS857 (Figure 4B), especially in slices expressing LTP.

Membrane depolarization has been shown to cause dephosphorylation of numerous endocytic proteins, including dynamin 1; therefore, the event is thought to facilitate the participation of these proteins in various synaptic functions.[10] The finding of a high overall level of pS857 in LTP slices is counterintuitive. This apparent paradox was resolved when the cellular distribution of pS857 dynamin 1xa in the hippocampus was analyzed. Phosphorylated dynamin 1xa was found primarily in the soma and throughout the entire length of apical dendrites in resting CA1 pyramidal neurons (Figure 6). HFS promoted pS857 dephosphorylation in an apparent all-or-nothing fashion. It caused full dephosphorylation in most neurons but left a few cells essentially untouched. The unaffected neurons are likely cells that happened to escape the brief stimulation. On the other hand, the distribution of dynamin 1xa pS857 in LTP-expressing pyramidal neurons was distinctly different from that of resting and HFS-stimulated slices (Figure 6B). The staining reveals the highly localized removal of pS857 in distal apical dendrites in LTP slices. Distal apical dendrites form synapses directly with the impinging axons of Schaffer collaterals, which conduct the synaptic transmission that originated from the CA3 region of hippocampus where electric stimulation was applied. Because all LTP slices were previously exposed to HFS, it is rational to suggest that the pattern of pS857 distribution in LTP slices evolved from that seen in slices stimulated with only HFS. As no dynamin 1 relocation is evident during stimulation (Figure 6B, Hudy 1), the pattern of pS857 dynamin 1xa distribution in the LTP slices must result from dynamin 1xa rephosphorylation, except in the distal apical dendrites. Our experiments revealed that HFS+, with a period of LFS following HFS, clearly influences both the dephosphorylation and rephosphorylation of dynamin. The equilibrium between these two processes is likely to be dependent on specific patterns of neuronal activation and is likely critical for synaptic function. To determine the dynamics of dynamin phosphorylation, its involvement in synaptic transmission, and its dependence on glutamatergic receptor activation, we employed HFS+, which affects both processes and mimics the in vivo environment, where hippocampal neurons not only fire spontaneously but also are activated by other brain structures with different frequencies. As a whole, rephosphorylation explains the overall higher level of pS857 in HFS+-stimulated than in HFS-stimulated slices (Figure 4B). The localized dephosphorylation of pS857 dynamin 1xa further affirms that pS857 is indeed dephosphorylated in response to stimulation from the Schaffer collaterals. However, it is surprising to learn that only a small fraction of total cellular dynamin 1xa is dephosphorylated in response to stimulation during LTP. Our findings with dynamin 1 S857 suggest that many phosphorylation-regulated endocytic

accessory proteins[10,11] may evoke a similar mechanism for controlling their activity.

As Ca^{2+} is required for pS857 dephosphorylation, the full-scale removal of pS857 in most HFS-stimulated neurons suggests a mechanism in which HFS induces a global Ca^{2+} influx in the affected neurons. Switching from HFS to LFS apparently limits Ca^{2+} influx to only restricted areas. An increase in Ca^{2+} levels in distal areas of apical dendrites of CA1 pyramidal neurons during Schaffer collateral stimulation has been well-documented.[37,38] The areas showing elevated levels of Ca^{2+} correspond spatially to the areas where pS857 dynamin 1xa is dephosphorylated during LTP. The rise and fall of the cytoplasmic level of Ca^{2+} in response to stimulation is extremely rapid.[37,38] Nevertheless, dynamin 1xa dephosphorylation was observed in stimulated slices. This finding may be attributed to the relatively slow rate of dynamin rephosphorylation as compared to that of dephosphorylation,[39] which allows the elevated concentration of cytoplasmic Ca^{2+} to be preserved in the state of dynamin 1 dephosphorylation. The NMDA receptor-mediated Ca^{2+} influx is considered to be the triggering event leading to LTP.[40] However, it appears that the Ca^{2+} influx involved in pS857 dephosphorylation during LTP is facilitated primarily by AMPA/kainate receptors rather than NMDA receptors (Figure 5). Several possible mechanisms, including release of Ca^{2+} from internal stores or Ca^{2+} influx through voltage-gated Ca^{2+} channels or Ca^{2+}-permeable AMPA receptors, may account for the AMPA/kainate receptor-facilitated Ca^{2+} influx[41−43] that leads to pS857 dephosphorylation. Attempts were made to measure calcineurin activity in slices subjected to different types of stimulation using a commercial calcineurin phosphatase assay kit (Enzo Life Sciences); however, we failed to detect any differences in activity between resting, HFS, and LTP slices. Changes in calcineurin activity caused by rapid calcium ion flux may be difficult to measure.

DYRK1A phosphorylation regulates the binding of dynamin 1 to several SH3 domain-containing proteins, such as amphiphysin 1, endophilin 1, and Grb 2 in vitro.[13,15] These interactions are necessary for assembling the large protein complexes required for endocytosis.[11] Although only the dynamin 1xa isoforms contain the primary DYRK1A phosphorylation site, S857, our results demonstrate that the level of binding of amphiphysin 1 to both dynamin 1xa and dynamin 1xb isoforms is reduced in parallel by DYRK1A phosphorylation (Figure 3A). This in vitro finding together with the co-IP of dynamin 1xa and 1xb isoforms (Figure 4B) suggests a model in which the dynamin 1xa and 1xb isoforms are co-assembled into heterologous complexes and regulated together as a unit by the embedded 1xa isoforms. Co-assembly of dynamin 1 and 2 as heterologous complexes has been demonstrated,[31] and the example of calcineurin further suggests that a factor recruited specifically by a type of dynamin 1 isoforms can coregulate all dynamins in the complex.[44] However, it should be pointed out that, besides S857, DYRK1A may also phosphorylate additional residues in the dynamin 1 PRD, such as S778 and S795.[15] These residues are present in both dynamin 1xa and 1xb isoforms. Alternatively, DYRK1A may phosphorylate these residues on dynamin 1xb directly and alter the binding of dynamin 1xb to amphiphysin as shown in Figure 3A. This possibility has not yet been fully examined. Analysis of dynamin phosphorylation at S857 has largely been overlooked until recently.[29] This may be due to the fact that synaptosomes, which have traditionally been used for dynamin phosphorylation investigation, can support only a minor level of S857 phosphorylation (Figure 2D).[28,29] The inability to support substantial S857 phosphorylation levels excludes synaptosomes as a suitable system for studying the consequences of dynamin 1 S857 phosphorylation.

DYRK1A efficiently phosphorylates dynamin 1xa at S857 in vitro.[15] This kinase appears to be the best candidate for supporting dynamin 1xa S857 phosphorylation in vivo, but its role has yet to be fully established. The gene for DYRK1A is located on human chromosome 21, and its level of expression is elevated in Down syndrome.[45] It is possible that gene dosage overexpression of DYRK1A and RCAN1, a chromosome 21-encoded specific calcineurin inhibitor,[46,47] in Down syndrome might synergistically interfere with phosphorylation regulation,[48] which might in turn disrupt the functional cycle of many proteins coregulated by DYRK1A and calcineurin.[49] Although no specific Down syndrome phenotype has been associated with the DYRK1A−RCAN1 imbalance so far,[50] this mechanism apparently causes elevated levels of phosphorylation of the transcription nuclear factor of activated T-cells and consequent alteration in NFAT-regulated gene expression.[51] Here, we illustrate that dynamin 1xa S857 phosphorylation is another potential system susceptible to the DYRK1A−RCAN1 imbalance. Because S857 of dynamin 1xa is already highly phosphorylated in vivo under normal conditions, the effect of such a gene imbalance would more likely influence the kinetics rather than the equilibrium of S857 phosphorylation.

■ ASSOCIATED CONTENT

Supporting Information

Subcellular distributions of pS857 dynamin 1xa (3D3) and dynamin 1xa (Hudy 1) in differentiated HN2-5 cells (Figure S1), immunological assays with pre-absorbed antibody 3D3 (Figure S2), and distributions of pS857 dynamin 1xa in the CA1 region of stimulated hippocampus (Figure S3). This material is available free of charge via the Internet at http://pubs.acs.org.

■ AUTHOR INFORMATION

Corresponding Author

*Department of Molecular Biology, New York State Institute for Basic Research in Developmental Disabilities, 1050 Forest Hill Rd., Staten Island, NY 10314. Telephone: (718) 494-5337. Fax: (718) 494-5905. E-mail: yuwen.hwang@csi.cuny.edu.

Present Addresses

[‖]Department of Hematology/Medical Oncology, Weill Cornell Medical College, 1300 York Ave., New York, NY 10021.

[⊥]Shandong Provincial Key Laboratory of Microbial Engineering, Shandong Polytechnic University, Jinan, Shandong 250353, China.

Funding

This work is supported in part by the New York State Office for People with Developmental Disabilities, the Jerome Lejeune Foundation (France, Y.-W.H.), and National Institutes of Health Grant HD 43960 to J.W.

Notes

The authors declare no competing financial interest.

■ ACKNOWLEDGMENTS

We are grateful to Richard B. Vallee of Columbia University (New York, NY) for kindly providing anti-dynamin 1xb antibody. We thank David L. Miller, Noriko Murakami, Carl Dobkin, and Kevin Hwang for critical reading of the

manuscript. We also thank Robert Freeland and Michael Flory for help with statistical analysis and Kevin Hwang for drawing the graphic for the table of contents.

■ ABBREVIATIONS

APV, D-2-amino-5-phosphonopentanoic acid; BAPTA/AM, 1,2-bis(*o*-aminophenoxy)ethane-*N*,*N*,*N*′,*N*′-tetraacetic acid, tetraacetoxymethyl ester; BTE, brain Triton extract; CA, cornu ammonis; Cdk5, cyclin-dependent kinase 5; CNQX, 6-cyano-7-nitroquinoxaline-2,3-dione; DYRK1A, dual-specificity tyrosine phosphorylation-regulated kinase 1A; GST, glutathione *S*-transferase; HFS, high-frequency stimulation; KYA, kynurenic acid; LFS, low-frequency stimulation; LTP, long-term potentiation; PRD, proline-rich domain; pS857, phospho-serine 857; RCAN1, regulator of calcineurin 1.

■ REFERENCES

(1) Praefcke, G. J., and McMahon, H. T. (2004) The dynamin superfamily: Universal membrane tubulation and fission molecules? *Nat. Rev. Mol. Cell Biol. 5*, 133−147.

(2) Hinshaw, J. E., and Schmid, S. L. (1995) Dynamin self-assembles into rings suggesting a mechanism for coated vesicle budding. *Nature 374*, 190−192.

(3) Takei, K., McPherson, P. S., Schmid, S. L., and De Camilli, P. (1995) Tubular membrane invaginations coated by dynamin rings are induced by GTP-γS in nerve terminals. *Nature 374*, 186−190.

(4) Macia, E., Ehrlich, M., Massol, R., Boucrot, E., Brunner, C., and Kirchhausen, T. (2006) Dynasore, a cell-permeable inhibitor of dynamin. *Dev. Cell 10*, 839−850.

(5) Roux, A., Uyhazi, K., Frost, A., and De Camilli, P. (2006) GTP-dependent twisting of dynamin implicates constriction and tension in membrane fission. *Nature 441*, 528−531.

(6) Sontag, J. M., Fykse, E. M., Ushkaryov, Y., Liu, J. P., Robinson, P. J., and Südhof, T. C. (1994) Differential expression and regulation of multiple dynamins. *J. Biol. Chem. 269*, 4547−4554.

(7) Okamoto, P. M., Herskovits, J. S., and Vallee, R. B. (1997) Role of the basic, proline-rich region of dynamin in Src homology 3 domain binding and endocytosis. *J. Biol. Chem. 272*, 11629−11635.

(8) Cao, H., Garcia, F., and McNiven, M. A. (1998) Differential Distribution of Dynamin Isoforms in Mammalian Cells. *Mol. Biol. Cell 9*, 2595−2609.

(9) Ferguson, S. M., Brasnjo, G., Hayashi, M., Wolfel, M., Collesi, C., Giovedi, S., Raimondi, A., Gong, L. W., Ariel, P., Paradise, S., O'Toole, E., Flavell, R., Cremona, O., Miesenbock, G., Ryan, T. A., and De Camilli, P. (2007) A selective activity-dependent requirement for dynamin 1 in synaptic vesicle endocytosis. *Science 316*, 570−574.

(10) Cousin, M. A., and Robinson, P. J. (2001) The dephosphins: Dephosphorylation by calcineurin triggers synaptic vesicle endocytosis. *Trends Neurosci. 24*, 659−665.

(11) Slepnev, V. I., and De Camilli, P. (2000) Accessory factors in clathrin-dependent synaptic vesicle endocytosis. *Nat. Rev. Neurosci. 1*, 161−172.

(12) Slepnev, V. I., Ochoa, G. C., Butler, M. H., Grabs, D., and De Camilli, P. (1998) Role of phosphorylation in regulation of the assembly of endocytic coat complexes. *Science 281*, 821−824.

(13) Chen-Hwang, M. C., Chen, H. R., Elzinga, M., and Hwang, Y. W. (2002) Dynamin is a minibrain kinase/dual specificity Yak1-related kinase 1A substrate. *J. Biol. Chem. 277*, 17597−17604.

(14) Tomizawa, K., Sunada, S., Lu, Y. F., Oda, Y., Kinuta, M., Ohshima, T., Saito, T., Wei, F. Y., Matsushita, M., Li, S. T., Tsutsui, K., Hisanaga, S., Mikoshiba, K., Takei, K., and Matsui, H. (2003) Cophosphorylation of amphiphysin I and dynamin I by Cdk5 regulates clathrin-mediated endocytosis of synaptic vesicles. *J. Cell Biol. 163*, 813−824.

(15) Huang, Y., Chen-Hwang, M. C., Dolios, G., Murakami, N., Padovan, J., Wang, R., and Hwang, Y. W. (2004) Mnbk/Dyrk1A Phosphorylation Regulates the Interaction of Dynamin 1with SH3 Domain-Containing Proteins. *Biochemistry 43*, 10173−10185.

(16) Anggono, V., Smillie, K. J., Graham, M. E., Valova, V. A., Cousin, M. A., and Robinson, P. J. (2006) Syndapin I is the phosphorylation-regulated dynamin I partner in synaptic vesicle endocytosis. *Nat. Neurosci. 9*, 752−760.

(17) Marks, B., and McMahon, H. T. (1998) Calcium triggers calcineurin-dependent synaptic vesicle recycling in mammalian nerve terminals. *Curr. Biol. 8*, 740−749.

(18) Tan, T. C., Valova, V. A., Malladi, C. S., Graham, M. E., Berven, L. A., Jupp, O. J., Hansra, G., McClure, S. J., Sarcevic, B., Boadle, R. A., Larsen, M. R., Cousin, M. A., and Robinson, P. J. (2003) Cdk5 is essential for synaptic vesicle endocytosis. *Nat. Cell Biol. 5*, 701−710.

(19) Clayton, E. L., Sue, N., Smillie, K. J., O'Leary, T., Bache, N., Cheung, G., Cole, A. R., Wyllie, D. J., Sutherland, C., Robinson, P. J., and Cousin, M. A. (2010) Dynamin I phosphorylation by GSK3 controls activity-dependent bulk endocytosis of synaptic vesicles. *Nat. Neurosci. 13*, 845−851.

(20) Clayton, E. L., Anggono, V., Smillie, K. J., Chau, N., Robinson, P. J., and Cousin, M. A. (2009) The phospho-dependent dynamin-syndapin interaction triggers activity-dependent bulk endocytosis of synaptic vesicles. *J. Neurosci. 29*, 7706−7717.

(21) Kim, Y., Park, J., Song, W. J., and Chang, S. (2010) Overexpression of Dyrk1A causes the defects in synaptic vesicle endocytosis. *Neurosignals 18*, 164−172.

(22) Xie, W., Ramakrishna, N., Wieraszko, A., and Hwang, Y. W. (2008) Promotion of neuronal plasticity by (−)-epigallocatechin-3-gallate. *Neurochem. Res. 33*, 776−783.

(23) Muzzolini, A., Bregola, G., Bianchi, C., Beani, L., and Simonato, M. (1997) Characterization of glutamate and [^{3}H]D-aspartate outflow from various in vitro preparations of the rat hippocampus. *Neurochem. Int. 31*, 113−124.

(24) Adayev, T., Chen-Hwang, M. C., Murakami, N., Wegiel, J., and Hwang, Y. W. (2006) Kinetic property of a MNB/DYRK1A mutant suitable for the elucidation of biochemical pathways. *Biochemistry 45*, 12011−12019.

(25) Bolte, S., and Cordelieres, F. P. (2006) A guided tour into subcellular colocalization analysis in light microscopy. *J. Microsc. (Oxford, U.K.) 224*, 213−232.

(26) Warnock, D. E., Terlecky, L. J., and Schmid, S. L. (1995) Dynamin GTPase is stimulated by crosslinking through the C-terminal proline-rich domain. *EMBO J. 14*, 1322−1328.

(27) Banerjee, P., Berry-Kravis, E., Bonafede-Chhabra, D., and Dawson, G. (1993) Heterologous expression of the serotonin 5-HT1A receptor in neural and non-neural cell lines. *Biochem. Biophys. Res. Commun. 192*, 104−110.

(28) Graham, M. E., Anggono, V., Bache, N., Larsen, M. R., Craft, G. E., and Robinson, P. J. (2007) The in vivo phosphorylation sites of rat brain dynamin I. *J. Biol. Chem. 282*, 14695−14707.

(29) Chan, L. S., Hansra, G., Robinson, P. J., and Graham, M. E. (2010) Differential phosphorylation of dynamin I isoforms in subcellular compartments demonstrates the hidden complexity of phosphoproteomes. *J. Proteome Res. 9*, 4028−4037.

(30) Muhlberg, A. B., Warnock, D. E., and Schmid, S. L. (1997) Domain structure and intramolecular regulation of dynamin GTPase. *EMBO J. 16*, 6676−6683.

(31) Okamoto, P. M., Tripet, B., Litowski, J., Hodges, R. S., and Vallee, R. B. (1999) Multiple distinct coiled-coils are involved in dynamin self-assembly. *J. Biol. Chem. 274*, 10277−10286.

(32) Bliss, T. V., and Collingridge, G. L. (1993) A synaptic model of memory: long-term potentiation in the hippocampus. *Nature 361*, 31−39.

(33) Isaac, J. T. (2003) Postsynaptic silent synapses: Evidence and mechanisms. *Neuropharmacology 45*, 450−460.

(34) Damke, H., Baba, T., Warnock, D. E., and Schmid, S. L. (1994) Induction of mutant dynamin specifically blocks endocytic coated vesicle formation. *J. Cell Biol. 127*, 915−934.

(35) Ochoa, G. C., Slepnev, V. I., Neff, L., Ringstad, N., Takei, K., Daniell, L., Kim, W., Cao, H., McNiven, M., Baron, R., and De Camilli,

P. (2000) A functional link between dynamin and the actin cytoskeleton at podosomes. *J. Cell Biol. 150*, 377−389.
(36) Huber, G., and Matus, A. (1984) Differences in the cellular distributions of two microtubule-associated proteins, MAP1 and MAP2, in rat brain. *J. Neurosci. 4*, 151−160.
(37) Regehr, W. G., and Tank, D. W. (1992) Calcium concentration dynamics produced by synaptic activation of CA1 hippocampal pyramidal cells. *J. Neurosci. 12*, 4202−4223.
(38) Alford, S., Frenguelli, B. G., Schofield, J. G., and Collingridge, G. L. (1993) Characterization of Ca^{2+} signals induced in hippocampal CA1 neurones by the synaptic activation of NMDA receptors. *J. Physiol. 469*, 693−716.
(39) Robinson, P. J., Liu, J. P., Powell, K. A., Fykse, E. M., and Südhof, T. C. (1994) Phosphorylation of dynamin I and synaptic-vesicle recycling. *Trends Neurosci. 17*, 348−353.
(40) Zucker, R. S. (1999) Calcium- and activity-dependent synaptic plasticity. *Curr. Opin. Neurobiol. 9*, 305−313.
(41) Sabatini, B. L., Maravall, M., and Svoboda, K. (2001) Ca^{2+} signaling in dendritic spines. *Curr. Opin. Neurobiol. 11*, 349−356.
(42) Thiagarajan, T. C., Lindskog, M., and Tsien, R. W. (2005) Adaptation to synaptic inactivity in hippocampal neurons. *Neuron 47*, 725−737.
(43) Plant, K., Pelkey, K. A., Bortolotto, Z. A., Morita, D., Terashima, A., McBain, C. J., Collingridge, G. L., and Isaac, J. T. (2006) Transient incorporation of native GluR2-lacking AMPA receptors during hippocampal long-term potentiation. *Nat. Neurosci. 9*, 602−604.
(44) Xue, J., Graham, M. E., Novelle, A. E., Sue, N., Gray, N., McNiven, M. A., Smillie, K. J., Cousin, M. A., and Robinson, P. J. (2011) Calcineurin selectively docks with the dynamin Ixb splice variant to regulate activity-dependent bulk endocytosis. *J. Biol. Chem. 286*, 30295−30303.
(45) Dowjat, W. K., Adayev, T., Kuchna, I., Nowicki, K., Palminiello, S., Hwang, Y. W., and Wegiel, J. (2007) Trisomy-driven over-expression of DYRK1A kinase in the brain of subjects with Down syndrome. *Neurosci. Lett. 413*, 77−81.
(46) Fuentes, J. J., Genesca, L., Kingsbury, T. J., Cunningham, K. W., Perez-Riba, M., Estivill, X., and de la Luna, S. (2000) DSCR1, overexpressed in Down syndrome, is an inhibitor of calcineurin-mediated signaling pathways. *Hum. Mol. Genet. 9*, 1681−1690.
(47) Rothermel, B., Vega, R. B., Yang, J., Wu, H., Bassel-Duby, R., and Williams, R. S. (2000) A protein encoded within the Down syndrome critical region is enriched in striated muscles and inhibits calcineurin signaling. *J. Biol. Chem. 275*, 8719−8725.
(48) Jung, M. S., Park, J. H., Ryu, Y. S., Choi, S. H., Yoon, S. H., Kwen, M. Y., Oh, J. Y., Song, W. J., and Chung, S. H. (2011) Regulation of RCAN1 Protein Activity by Dyrk1A Protein-mediated Phosphorylation. *J. Biol. Chem. 286*, 40401−40412.
(49) Gardiner, K. (2003) Predicting pathway perturbations in Down syndrome. *J. Neural. Transm., Suppl. 67*, 21−37.
(50) Korbel, J. O., Tirosh-Wagner, T., Urban, A. E., Chen, X. N., Kasowski, M., Dai, L., Grubert, F., Erdman, C., Gao, M. C., Lange, K., Sobel, E. M., Barlow, G. M., Aylsworth, A. S., Carpenter, N. J., Clark, R. D., Cohen, M. Y., Doran, E., Falik-Zaccai, T., Lewin, S. O., Lott, I. T., McGillivray, B. C., Moeschler, J. B., Pettenati, M. J., Pueschel, S. M., Rao, K. W., Shaffer, L. G., Shohat, M., Van Riper, A. J., Warburton, D., Weissman, S., Gerstein, M. B., Snyder, M., and Korenberg, J. R. (2009) The genetic architecture of Down syndrome phenotypes revealed by high-resolution analysis of human segmental trisomies. *Proc. Natl. Acad. Sci. U.S.A. 106*, 12031−12036.
(51) Arron, J. R., Winslow, M. M., Polleri, A., Chang, C. P., Wu, H., Gao, X., Neilson, J. R., Chen, L., Heit, J. J., Kim, S. K., Yamasaki, N., Miyakawa, T., Francke, U., Graef, I. A., and Crabtree, G. R. (2006) NFAT dysregulation by increased dosage of DSCR1 and DYRK1A on chromosome 21. *Nature 441*, 595−600.